

## Remote monitoring ice velocities of the polar record and the Dark Glaciers

Sun Jiabing(孙家柄), Zhou Junqi(周军其), Huo Dongmin(霍东民) and Sun Zhaohui(孙朝辉)  
*School of remote sensing and informatics, Wuhan University, Wuhan 430079, China*

Received February 8, 2003

**Abstract** Measurement of ice velocities of the Antarctic glaciers is very important for studies on Antarctic ice and snow mass balance. The polar area environmental change and its influences on the global environment. Conventional methods may be used for measuring the ice velocities, but they suffer from severe weather conditions in the Polar areas. Use of satellite multi-spectral and multi-temporal images makes it easier to measure the velocities of the glacier movements. This paper discusses a new method for monitoring the glacial change by means of multi-temporal satellite images. Temporal remotely sensed images in the Ingrid Christensen coast were processed with respect to geometric rectification, registration and overlay. The average ice velocities of the Polar Record Glacier and the Dark Glacier were then calculated, with the changing characteristics analyzed and evaluated. The advantages of the method reported here include promise of all-weather operation and potentials of dynamic monitoring through suitable selection of temporal satellite images.

**Key words** The Ingrid Christensen Coast, multi-temporal remotely sensed images, the Polar Record Glacier, the Dark Glacier, glacial ice velocities.

### 1 Introduction

The measurement of ice velocities and fluxes of the Antarctic glaciers is very significant to the study on the Antarctic ice and snow mass balance, the Antarctic environment change and its influence on the global environment. There are many kinds of methods measuring the ice velocities at present. The first method is measuring it on spot, including traditional measurement and local measurement with GPS (Manson *et al.* 2000). This method has high precise but it is very dangerous under the Antarctic climate and environment especially in the occurrence of squall and ice crack leading to the destruction of people and device (Abdalati and Krabill 1999). In order to keep the staffs safe, flag of measurement is set standing by itself at Glacier, and observed with measuring angle or intersection of distance periodically; meantime GPS receiver is set at Glacier, difference calculation with the stable station is done to get the velocity. By the former two methods, the devices are likely to be extruded and destroyed or fall into the ice crack when glacier moves. The power provision of receiver device of GPS is once more a difficult problem. The second method is aerophotographing in periodic, then the changeable glacier is observed with photogrammetry

(Brecher 1986; Krimmel 1987). But the method is influenced by climate and condition in aerophotography, moreover, there had been difficult that the reflection of ice surface is too strong and the ground control points is difficult to be measured. The third method is to use aero laser altimeter to monitor the velocity of glacier, it was tested in Greenland (Abdalati 1999). The application of the third is also limited by the climate and environment in Polar as arcophotography. The fourth method is to use interference synthetic aperture antenna radar (INSAR) such as interference images of the same area acquired by ERS-1 and ERS-2 satellite of European Space Bureau to measure the velocity of glacier moving (Joughin *et al.* 1995; Rignot *et al.* 1995; Kwok and Fahnestock 1996). In the last method satellite multi-spectral and multi-temporal images were applied to measure the velocity and fluxes of the glacier moving (Scambos *et al.* 1992; Scambos and Bindshadler 1993). This method has the advantage of safety and could choose the suitable temporal satellite images to monitor and analyze in general.

There are tens of glaciers that flow to seacoast from the land at The Ingrid Christensen Coast in east-southern polar princess Elizabeth land. Among the glaciers, the one nearest to Zhongshan station is Dark Glacier which lies at Larsemann Hills in the east of Mirror Peninsula, ice crack occurred in 1988. The broken glacier lingua, which lies in front of the glacier, flows to sea and forms many icebergs. The largest glacier is Polar Record Glacier, which is 50 Km distance from the west southern of Larsemann Hills. Its width is above 25 km. There are three research stations, Chinese, Russian and Australian in Mirror Peninsula, yet the study on the velocity and fluxes of the two glaciers had not been reported. This paper reports the study which has monitored dynamically the Polar Record Glacier and Dark Glacier with the satellite images acquired in three dates and with three different sensors in the same area and good result has been gotten.

## 2 Data and pre-processing

In order to monitor glacier movements it is necessary to acquire satellite images in different time, images acquiring with Landsat MSS and TM should be operated in a cloud-free condition. Although Radarsat does not suffer from cloud cover, the right side-looking of SAR must be switched to left side-looking, as was done by Radarsat's polar missions from 9<sup>th</sup> September 1997 to 11<sup>th</sup> March 1998. The data set used in this study includes Landsat-1 MSS, Landsat-4 TM and Radarsat SAR images, are shown in Table 1.

Table 1. The satellite data set

Satellites and sensors	Acquisition dates	Resolutio ( m )	Bands	Wave lengths
Landsat-1 MSS	4 th February, 1973	80	MSS 7	0.8-1.1 $\mu$
Landsat-4 TM	20 th January 1990	30	TM4	0.76-0.90 $\mu$
Radarsat SAR	14 th September 1997	50	C band	5.6 cm

Shape and texture may be useful indicators of glacier movement. The NR bands of Landsat MSS and TM were selected for display of ice, and the Radarsat SAR image depicts texture better with the difference enhanced between the ice surface and seawater. A three-segment contrast stretch was used to stretch middle hue:

$$I' = \begin{cases} A_1 I + B_1 & \text{for } a < I < b \\ A_2 I + B_2 & \text{for } b < I < c \\ A_3 I + B_3 & \text{for } c < I < d \end{cases} \quad (1)$$

where  $a, b, c$  and  $d$  are threshold parameters, as shown in Figure 1.

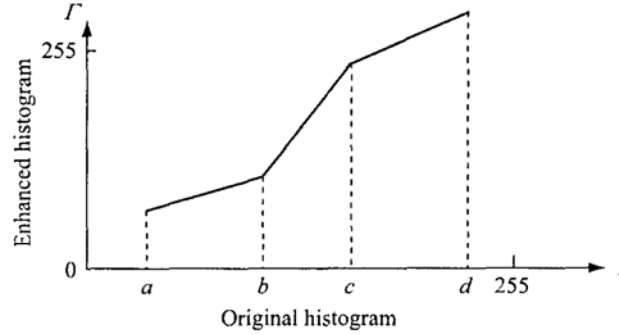


Fig. 1. Piecewise linear contrast stretch with three segments.

Laplacian algorithm was used for developing the enhancement of glacier shapes and textures in the study area:

$$g(x, y) = \nabla^2 f(x, y) \quad (2)$$

In practice, image differential is usually performed within a 3 by 3 window:

$$\nabla^2 f(x, y) = f(x+1, y) + f(x-1, y) + f(x, y+1) + f(x, y-1) - 4f(x, y) \quad (3)$$

The enhanced image is derived by addition of the differential and the original images:

$$g'(x, y) = 2f(x, y) + g(x, y) \quad (4)$$

The Landsat TM image with 30 m resolution was regarded as the basis to rectify other images with Gauss projection. Seven ground control points (GCPs) distributed over the Larsemann Hill were measured with respect to altazimuth and laser. Its geodesic and image coordinate are shown in Table 2.

Table 2. The geodetic and image coordinate of ground control points

GCPs	Image coordinate		Geodetic coordinate(m)	
	L	P	Y	X
1	2934	3226	2289479	514754
2	3003	3323	2286627	516334
3	3017	3295	2286617	515472
4	3052	3291	2285773	514960
5	3007	3225	2287694	513850
6	2976	3181	2289026	513099
7	3100	3202	2285695	512208

First-order polynomials were used to geo-reference images:

$$\begin{aligned} X &= a_0 + a_1 L + a_2 P \\ Y &= b_0 + b_1 L + b_2 P \end{aligned} \quad (5)$$

The coefficients of polynomial were calculated via least squares adjustment, with normal equation being formulated as:

$$\Delta = [A^T A]^{-1} [A^T Y] \quad (6)$$

Positional accuracy was assessed using standard error in X or Y coordinates:

$$\delta = \sqrt{\frac{[VV]}{m-f}} \quad (7)$$

The adjusted residual errors of ground control points are shown in Table 3.

Table 3. Residual errors (unit: meter)

NO.	1	2	3	4	5	6	7	Total residual errors
$\delta X$	-15.8	15.6	-19.8	19.4	2.9	-12.4	10.1	12.5
$\delta Y$	21.3	-0.8	-7.6	-24.3	-14.4	-3.0	-3.8	12.3

Bilinear interpolation is applied for image resampling:

$$p = \sum_{i=1}^2 \sum_{j=1}^2 W_{ij} I_{ij} \quad (8)$$

For this study, the resample pixel size was 50m, Landsat MSS and Radarsat SAR image was added to the rectified Landsat TM image, respectively. Objects for image matching were chosen from those that changed little, especially the small and large peninsula and islands at the Larsemann Hill. The resultant image size is 80 km by 80 km.

The Landsat MSS image was matched with the TM image:

$$\begin{aligned} L_T &= a_{m0} + a_{m1} L_m + a_{a2} P_m \\ P_T &= b_{m0} + b_{m1} L_m + b_{a2} P_m \end{aligned} \quad (9)$$

As Radarsat SAR is slant ranging projection with quadratic distortion, quadratic polynomial is used to match it to the Landsat TM image:

$$\begin{aligned} L_T &= a_{s0} + a_{s1} L_s + a_{s2} P_s + a_{s3} L_s^2 + a_{s4} L_s P_s + a_{s5} P_s^2 \\ P_T &= b_{s0} + b_{s1} L_s + b_{s2} P_s + b_{s3} L_s^2 + b_{s4} L_s P_s + b_{s5} P_s^2 \end{aligned} \quad (10)$$

### 3 Interpretation and measurement of glaciers

The end of the Polar Record Glacier is stretching continuously into sea about 50 km (Prydz Bay) and floating on the sea, as demonstrated in the Landsat MSS image in Figure 2. As the glacier flowing outward, the surface of sea could not sustain the weight of the large glacier, and there was a collapse in 1990, resulting in a large iceberg of three times the size of Wuhan (the south-east part is shown in the Landsat TM image, Figure 3). Sliding outward and collapsing afterwards, the iceberg seen in the 1997 Landsat TM image has an area of twice that of Wuhan, about 360 km<sup>2</sup>.

The icebergs usually stay in the gulf because they are too large and almost frozen all over the year and the coast is shallow. The Polar Record Glacier continuously flow out with constant speed: there is a gap between the icebergs seen in Figure 3 and the front edge of Polar Record Glacier, the shape of which is identical as of the icebergs seen in Figure 4.

The front edge of iceberg of Radarsat SAR image is different from that of the Landsat MSS image, but their textures are still similar: the peak of glacier front edge in 1973 could be found, shapes remain the same for the icebergs seen in the images of 1990 and 1997. Glacier had stretched 6 km from 1990 to 1997, while the glaciers had stretched into sea 50 km from 1973. It can be seen that there is no ice collapse in 7 years, so the velocity and

fluxes of the Polar Record Glacier can be calculated.



Fig. 2. The Landsat-1 MSS image acquired on 4<sup>th</sup> February 1973 (resolution: 80 m, gridline interval: 10 by 10 km).



Fig. 3. The Landsat-4 TM image acquired on 20<sup>th</sup> January 1990 (resolution: 30 m, gridline interval: 10 by 10 km).

The Dark Glacier lies in the east of the Mirror peninsula, The width of which is about 3 km and is smaller than Polar Record Glacier, and is close to the three research stations of Russia, Austria and China with their research ships anchored at the gulf every year.

As images matched in each other, it is possible to overlay the images, with the positions of changeable and unchangeable objects identified. For the Polar Record Glacier, when Landsat MSS image is overlaid to the Landsat TM image acquired in 1990, it is easy to see the lines of glacier movements (Figure 5). The edges of lingua at Polar Record Glacier and Dark Glacier are identified from overlaying the Landsat TM image and the Radarsat SAR image (Figure 6). The distances between matched points can be measured. Since the large iceberg is flowing away from glacier before 1990, the distance between the matched points from 1973 to 1990 should be minus the interval distance, retrieving the real glacier movement. As there was no ice-cracking after 1990, the distance of matched points is equal to



Fig. 4. The Radarsat-1 SAR image acquired on 14<sup>th</sup> September 1997 (resolution: 50 m, gridline interval: 10 by 10 km).

the distance of glacier movement.



Fig. 5. The outline of the Polar Record Glacier in 1973, overlaid with the image acquired in 1990.



Fig. 6. The outline of the Polar Record Glacier and the Dark Glacier in 1990, overlaid with the image acquired in 1997.

The velocity calculation formula is:

$$V = D/\Delta t \quad (11)$$

where  $D$  is a real distance of glacier, and  $\Delta t$  is the difference of two images acquiring time.

Table 4. The motion distance and average velocity during 1973 – 1990

	Time periods	Distance(m)	Annual average(m)	Daily average(m)
Polar Record Glacier	Feb. 4, 1973- Jan. 20, 1990	13258.58	781.76 m	2.14 m
Polar Record Glacier	Jan. 20, 1990- Sep. 14, 1997	6380.635	834.1 m	2.29 m
Dark Glacier	Jan. 20, 1990- Sep. 14, 1997	1457.74	190.55 m	0.52 m

As shown in table 4, the average velocity, fluxes of Polar Record Glacier is 781.76 m per year from 1973 to 1990, the average velocity is 2.14 m a day. The average velocity is 834.1 m per year from 1990 to 1997, the average velocity is 2.29 m a day, consequently, the average velocity is equal. The average velocity is higher in 1990 than that in 1997, the reason is that the lingua of glacier was longer, and flowed more slowly between 1973 to 1990. The Polar Record Glacier broken in 1990, the lingua got shorter, so the moving velocity rose. With the same method, the average velocity of Dark Glacier moving is 190.55 m a year, the day average velocity is 0.52 m. It is smaller than that of Polar Record Glacier, but the average stretch outward 190 m is considerable.

## References

- Abdalatic W, Blrabill W (1999): Calculation of ice velocities in the Jakobshavn Isbraearea using laser altimetry. *Remote Sensing of Environment*, 67;194-204.
- Brecher HH (1986): Surface velocity determination on large potar glaciers by aerialphotogrammetry. *Annals of Glacier*, 8; 22-26.
- Joughin IR *et. al.* (1995): Observation of ice-sheet motion in Greenland usingsatelliteradar interometry. *Geophys Research Letters*, 22;571-574.
- Krimmel RM (1987): Columbia Glacier, Alaska; photogrammetry data set 1981-82 and1984-85, USGS open file report, 87-219, U. S. Geological Survey, 104.
- Kwok R, Fahnestock MA (1996): Ice sheet motion and topography from radarinterferometer. *IEEE Transactions on Geosciences and Remote Sensing*, GE-34; 88-97.
- Manson R *et al.* (2000): Ice velocities of the Lambert from static GPS observations. *EarthPlanets Space*, 00, 001-006.
- Rignot E. *et. al.* (1995): Ice flow dynamics of the Greenland ice sheet from SARinterrrrrferometry. *Geophysics Research Letters*, 22; 575-578.
- Scambos TA *et. al.* ( 1992): Application of image cross-correlation to the measurement of glacier velocity using satellite image data. *Remote Sensing of Environment*, 42; 177-186.
- Scambos TA, Bindshadler RA (1993): Complex ice stream flow revealed bysequential satellite imagery. *Annats of Glacier*, 17;177-182.